JOC Article

Chair to Boat Interconversion and Face to Face Interactions in Isomeric Aryl-Substituted Perhydrocyclopentaquinolizines

Lodovico Lunazzi,[§] Andrea Mazzanti,*[,§] Shaik Rafi,[¶] and H. Surya Prakash Rao[¶]

Department of Organic Chemistry "A. Mangini", University of Bologna, Viale Risorgimento, 4 Bologna 40136, Italy, and Department of Chemistry, Pondicherry University, Puducherry 605014 India

mazzand@ms.fci.unibo.it

Received October 8, 2007

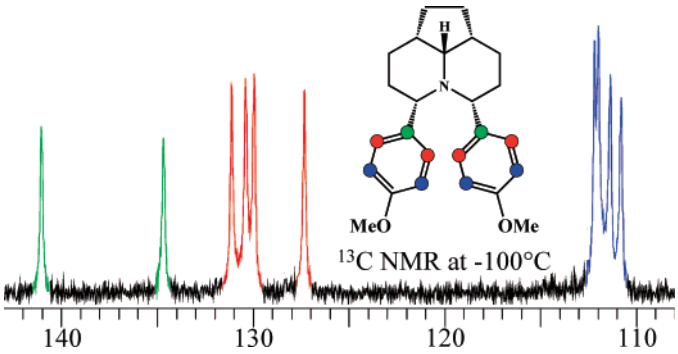

The structure and the conformation of the two isomeric 3,5-di(4-methoxyphenyl)perhydrocyclopenta[*ij*]-quinolizines **1** and **2** have been determined by a combination of NOE experiments, analysis of vicinal *J* coupling constants, and DFT computations. The two aryl rings were found to exhibit a face to face disposition, and variable-temperature NMR spectra allowed the determination of the corresponding rotation barriers, as well as chair to boat and nitrogen inversion processes of the quinolizine rings. The structure and the conformation of the two corresponding ammonium salts **1-H**$^+$ and **2-H**$^+$ were also obtained in solution by the same techniques: in addition, their solid-state structures were determined by X-ray diffraction.

Introduction

Aryl groups bonded to *peri* positions of a planar framework, like 1,8-disubstituted naphthalene, adopt a face to face (stacked) arrangement and display restricted rotation about the aryl naphthalene bond that, in particular cases, might have a sufficiently high barrier to produce configurationally stable *cis* and *trans* isomers.[1] A number of barriers for the interconversion of these types of isomers have been reported.[2] When the aryl substituents are not sufficiently large, stereolabile isomers (conformers) have often been observed and the corresponding interconversion barriers determined by variable-temperature NMR spectroscopy.[3] Heterocyclic rings bonded to the 1,8-positions of naphthalene displayed analogous features.[4] Barriers of this type were also determined in the case of aryl groups bonded, in a stacked arrangement, to other rigid frameworks such as anthracene,[5] cyclobutane,[6] and acenaphthene.[7]

Here we present a quite peculiar situation where two aryl rings are bonded to the less rigid framework of perhydrocy-

[§] University of Bologna.
[¶] Pondicherry University.

(1) Clough, J. D.; Roberts, J. D. *J. Am. Chem. Soc.* **1976**, *98*, 1018.
(2) (a) Cozzi, F.; Cinquini, M.; Annunziata, R.; Dwyer, T.; Siegel, J. S. *J. Am. Chem. Soc.* **1992**, *114*, 5729. (b) Cozzi, F.; Cinquini, M.; Annunziata, R.; Siegel, J. S. *J. Am. Chem. Soc.* **1993**, *115*, 5330. (c) Tumambac, G. E.; Wolf, C. *J. Org. Chem.* **2005**, *70*, 2930.
(3) (a) House, H. O.; Campbell, W. J.; Gil, M. *J. Org. Chem.* **1970**, *35*, 1815. (b) Anderson, J. E.; Cooksey, C. J. *Chem. Commun.* **1975**, 942. (c) Cosmo, R.; Sternhell, S. *Aust. J. Chem.* **1987**, *40*, 1107. (d) Cozzi, F.; Ponzini, F.; Annunziata, R.; Cinquini, M.; Siegel, J. S. *Angew. Chem., Int. Ed. Engl.* **1995**, *34*, 1019. (e) Thirsk, C.; Hawkes, G. E.; Kroemer, R. T.; Liedl, K. R.; Loerting, T.; Nasser, R.; Pritchard, R. G.; Steele, M.; Warren, J. E.; Whiting, A. *J. Chem. Soc., Perkin Trans. 2* **2002**, 1510.
(4) (a) Zoltewicz, J. A.; Maier, N. M.; Fabian, W. M. F. *J. Org. Chem.* **2006**, *71*, 7018. (b) Wolf, C.; Ghebremariam, B. T. *Tetrahedron: Asymmetry* **2002**, *13*, 1153. (c) Zoltewicz, J. A.; Maier, N. M.; Fabian, W. M. F. *Tetrahedron* **1996**, *52*, 8703. (d) Nakagawa, Y.; Honda, K.; Nakanishi, H. *Magn. Reson. Chem.* **1996**, *34*, 78.
(5) Lunazzi, L.; Mancinelli, M.; Mazzanti, A. *J. Org. Chem.* **2007**, *72*, 5391 and references quoted therein.
(6) Ben-Efraim, D. A.; Arad-Yellin, R. *J. Chem. Soc., Perkin Trans. 2* **1994**, 853.
(7) Lai, Y.-H.; Chen, P. *J. Chem. Soc., Perkin Trans. 2* **1989**, 1665.

10.1021/jo702172u CCC: $40.75
Published on Web 12/22/2007

SCHEME 1

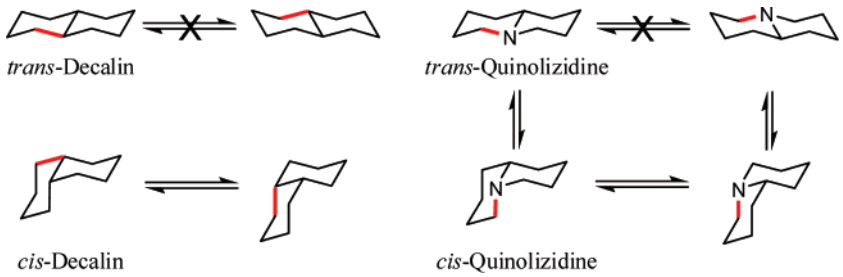

CHART 1

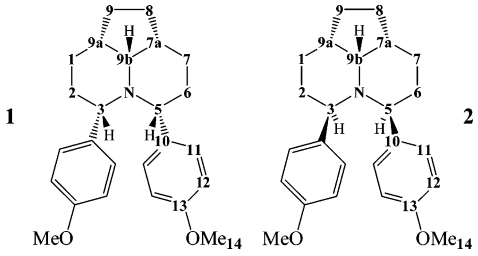

clopentaquinolizine[8] (see compounds **1** and **2** of Chart 1, where methoxy groups in the *para* position of the aryl rings serve to simplify NMR spectra). Thus, in addition to the rotation process involving these anisole substituents attached to a more flexible ring system, the inversion processes occurring within the perhydrocyclopentaquinolizine moiety should also be observed.

In the perhydroquinolizine (quinolizidine) framework, which is well-represented among many physiologically active alkaloids,[9] a nitrogen atom replaces the carbon C-4a of *cis*- or *trans*-decalins (perhydronaphthalenes), as displayed in Scheme 1. The framework of *trans*-decalin is locked, as it cannot invert to an alternative chair−chair system unless carbon−carbon bonds are broken and then rejoined;[10] on the contrary, *cis*-decalin can interconvert between two chair−chair conformations, even at ambient temperature. As shown in Scheme 1, and in contrast to the conformational rigidity of *trans*-decalin, the *trans*-quinolizidine can interconvert from one chair−chair conformation to other chair−chair conformations via *cis*-quinolizidine. This is possible since nitrogen inverts its configuration and, since this process is faster than chair-to-chair exchange in piperidines,[11] it is likely that *trans*-quinolizidines interconvert rapidly to another form at ambient temperature.[12] Equilibration of chair conformations in quinolizidines can be prevented by adding a bridging ring such as that of cyclopenta[*i*,*j*]quinolizidines **1** and **2** in Chart 1 or by blocking nitrogen inversion by conversion of the molecule to the corresponding ammonium salt, in effect making the system more similar to *trans*-decalins.

Dynamic NMR spectroscopic analysis can be used to evaluate the conformational changes involving, possibly, nitrogen inversion, ring inversion, and restricted rotation of the aryl rings in quinolizidines of the types **1** and **2**. Since the basic cyclopenta[*i*,*j*]quinolizidine structural motif is encountered in the structure of a number of complex alkaloids such as vallesamidine,[13] callichiline,[14] criophylline,[15] and schizozygine,[16] studies of the conformational dynamics involved in such systems can be quite useful from the point of view of structure−activity relationships.

Results and Discussion

Amines 1 and 2. The structure of amine **1** (Chart 1) was investigated by NOE experiments and was found to correspond to a *cis*,*cis* ring junction[8b] at the perhydrocyclopentaquinolizine moiety. As reported in Figure S1 of Supporting Information, irradiation of the triplet of H9b (at 2.88 ppm) yields NOE effects on the pair of hydrogens 3,5 (at 3.24 ppm), on the pair of hydrogens 7a,9a (at 2.28 ppm), and on the hydrogens 1,7 (at 1.71 and 1.55 ppm). On the contrary, NOE was not observed on H8,H9 (1.84 and 2.02 ppm) nor on the aromatic hydrogens. These results were further confirmed by the irradiation of the H3,H5 triplet.

A complete conformational search for this type of structure was carried out by molecular mechanics force field (MMFF) measurements,[17] and the two most stable conformers were subsequently minimized by DFT computations.[18] In Figure 1 (top left) is displayed the preferred conformation (its energy is

(8) (a) Rao, H. S. H.; Jeyalakshmi, K.; Senthilkumar, S. P. *Tetrahedron* **2002**, *58*, 2189. (b) It has to be pointed out that the nomenclatures for the perhydrocyclopentaquinolizine ring junctions displayed in Scheme 7 of ref 8a are in error and must be interchanged, that is, the picture called *trans*,*trans* is actually *cis*,*cis* and vice versa.

(9) *Alkaloids: Biochemistry, Ecology and Medicinal Applications*; Roberts, M. F., Wink, M., Eds.; Springer: New York, 1998.

(10) Eliel, E. L.; Wilen, S. H.; Mander, L. N. *Stereochemistry of Organic Compounds*; Wiley-Interscience: Kundli, 2003; pp 776−777.

(11) (a) Rubiralta, M.; Giralt, E.; Diez, A. *Piperidine: Structure, Preparation, Reactivity and Synthetic Applications of Piperidine and its Derivatives*; Elsevier: Amsterdam, 1991. (b) Anet, F. A. L.; Yavari, I. *J. Am. Chem. Soc*. **1977**, *99*, 2794.

(12) (a) Moyneh, T. M.; Schofield, K.; Jones, R. A.; Katritzky, A. R. *J. Chem. Soc.* **1962**, 2637. (b) Sugiura, M.; Sasaki, Y. *Chem. Pharm. Bull*. **1976**, *22*, 2988. (c) Lalonde, R. T.; Donvito, T. N. *Can. J. Chem*. **1974**, *52*, 3778. (d) Slough, G. A.; Han, F.; Lee, B. H. *Tetrahedron Lett.* **1999**, *40*, 3851 .

(13) Dickman, D. A.; Heathcock, C. A. *J. Am. Chem. Soc*. **1989**, *111*, 1528.

(14) Mcphail, A. T.; Poisson, J. *Tetrahedron* **1983**, *39*, 3629.

(15) Seok kam, T.; Yeng loh, K.; Chen, W. *J. Nat. Prod*. **1993**, *56*, 1865.

(16) Renner, U.; Kernweisz, P. *Experentia* **1963**, *19*, 244.

(17) MMFF, as implemented in *Titan 1.0.5*, Wavefunction Inc.: Irvine, CA. A Monte Carlo algorithm (version 1.0.3) was used for locating the global minima.

(18) Frisch, M. J.; Trucks, G. W.; Schlegel, H. B.; Scuseria, G. E.; Robb, M. A.; Cheeseman, J. R.; Montgomery, J. A., Jr.; Vreven, T.; Kudin, K. N.; Burant, J. C.; Millam, J. M.; Iyengar, S. S.; Tomasi, J.; Barone, V.; Mennucci, B.; Cossi, M.; Scalmani, G.; Rega, N.; Petersson, G. A.; Nakatsuji, H.; Hada, M.; Ehara, M.; Toyota, K.; Fukuda, R.; Hasegawa, J.; Ishida, M.; Nakajima, T.; Honda, Y.; Kitao, O.; Nakai, H.; Klene, M.; Li, X.; Knox, J. E.; Hratchian, H. P.; Cross, J. B.; Bakken, V.; Adamo, C.; Jaramillo, J.; Gomperts, R.; Stratmann, R. E.; Yazyev, O.; Austin, A. J.; Cammi, R.; Pomelli, C.; Ochterski, J. W.; Ayala, P. Y.; Morokuma, K.; Voth, G. A.; Salvador, P.; Dannenberg, J. J.; Zakrzewski, V. G.; Dapprich, S.; Daniels, A. D.; Strain, M. C.; Farkas, O.; Malick, D. K.; Rabuck, A. D.; Raghavachari, K.; Foresman, J. B.; Ortiz, J. V.; Cui, Q.; Baboul, A. G.; Clifford, S.; Cioslowski, J.; Stefanov, B. B.; Liu, G.; Liashenko, A.; Piskorz, P.; Komaromi, I.; Martin, R. L.; Fox, D. J.; Keith, T.; Al-Laham, M. A.; Peng, C. Y.; Nanayakkara, A.; Challacombe, M.; Gill, P. M. W.; Johnson, B.; Chen, W.; Wong, M. W.; Gonzalez, C.; Pople, J. A. *Gaussian 03*, revision D.01; Gaussian, Inc.: Wallingford, CT, 2004 (see Supporting Information).

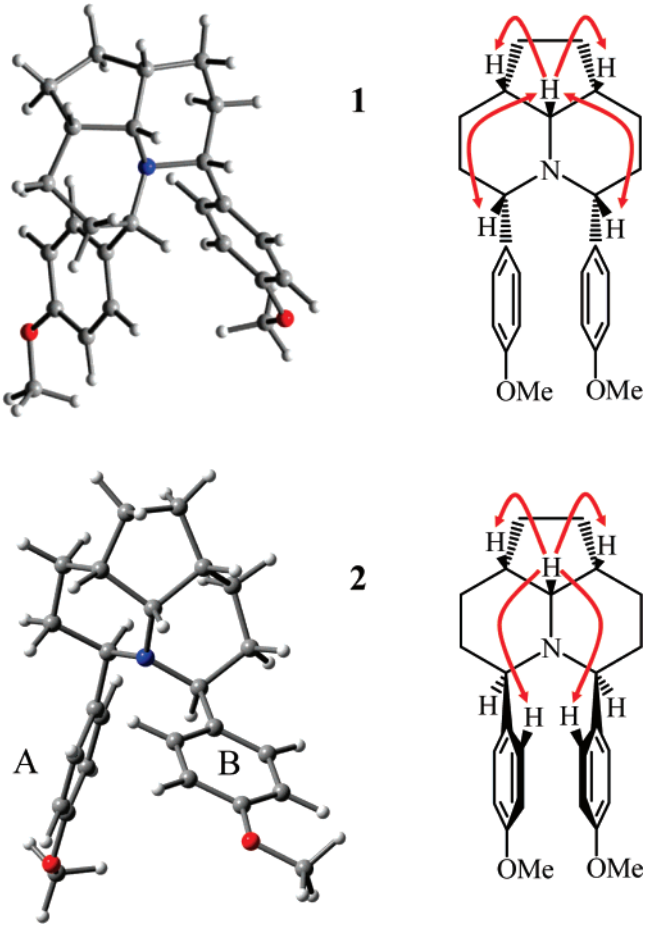

FIGURE 1. Top: DFT-computed structure (left) of the preferred conformer of **1** (arbitrarily selected as 3*S*,5*R*,7a*R*,9a*S*). The exchange with its mirror image yields a dynamic C_s symmetry (right) with the aryl rings *syn* to the five-membered ring (i.e., in the same average pseudoequatorial positions). Bottom: DFT-computed structure (left) of the preferred conformer of **2** (arbitrarily selected as 3*R*,5*S*,7a*R*,-9a*S*). The exchange with its mirror image yields a dynamic C_s symmetry (right) with the aryl rings *anti* to the five-membered ring (i.e., in the same average pseudoaxial positions). The arrows indicate the large NOE effects experimentally observed.

1.9 kcal mol^{-1} lower than that of the second most stable form where both the six-membered rings are chairs), where one of the two six-membered rings is a chair and the other is a twisted-boat.[19] Such a static conformer exists as two enantiomeric forms that interconvert rapidly at ambient temperature yielding a dynamic C_s symmetry which accounts for the equivalence of the pairs of the ^{13}C lines in the corresponding spectrum at 25 °C (Supporting Information).

The DFT computed H−C9b−C9a−H and H−C9b−C7a−H dihedral angles are 46 and 38°, respectively: when introduced

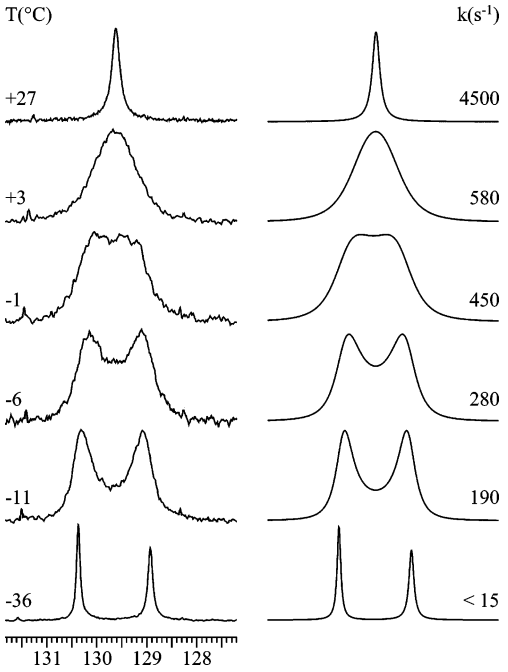

FIGURE 2. Left: Temperature dependence of the ^{13}C signal (150.8 MHz in CD_2Cl_2) of the aromatic carbons *meta* to the OMe group (position 11) of compound **1**. Right: Computer simulation with the rate constants reported.

in the Karplus equation,[20] they yield vicinal *J* couplings of 3.7 and 4.9 Hz. Due to the mentioned rapid interconversion at ambient temperature, the average *J* becomes 4.3 Hz. We also calculated these vicinal *J* couplings by making direct use of the DFT approach[18] (including the Fermi contact contribution), thus avoiding the application of the empirical Karplus equation: the values obtained in this way were found to be 4.6 and 5.6 Hz, yielding an average *J* coupling of 5.2 Hz. By taking into account the two theoretical approaches (that define a range of 4.3−5.2 Hz), we can predict a value of 4.7 ± 0.5 Hz for this *J* coupling (Table 1), which fits well with the experimental value (4.5 Hz).[21]

(19) The twist-boat conformation has been found to occur in a number of six-membered rings; see: (a) Bushweller, C. H. *J. Am. Chem. Soc*. **1969**, *91*, 6019. (b) Weiser, J.; Golan, O.; Fitjer, L.; Biali, S. E. *J. Org. Chem*. **1996**, *61*, 8277. (c) Gill, G.; Pawar, D. M.; Noe, E. A. *J. Org. Chem*. **2005**, *70*, 10726. (d) Thanikasalam, K.; Jeyaraman, R.; Panchanatheswaran, K.; Low, J. N.; Glidwell, C. *Acta Crystallogr*. **2006**, *C62*, o324.

(20) Karplus, M. *J. Am. Chem. Soc*. **1963**, *85*, 2870.

(21) Except for the presence of the two OMe groups, compound **1** corresponds to that indicated as **30** (amount 58%) in ref 8a (both have, in fact, very similar NMR parameters for the perhydrocyclopentaquinolizine moiety). On the basis of the present results, the structure of the latter should be therefore corrected and the same structure of compound **1** should be assigned.

(22) As often observed in conformational processes, the free energy of activation was found independent of temperature within the errors, indicating a negligible value of $\Delta S^{\ddagger}$. See, for instance: (a) Dondoni, A.; Lunazzi, L.; Giorgianni, P.; Macciantelli, D. *J. Org. Chem*. **1975**, *40*, 2979. (b) Hoogosian, S.; Bushweller, C. H.; Anderson, W. G.; Kigsley, G. *J. Phys. Chem*. **1976**, *80*, 643. (c) Lunazzi, L.; Cerioni, G.; Ingold, K. U. *J. Am. Chem. Soc*. **1976**, *98*, 7484. (d) Lunazzi, L.; Dondoni, A.; Barbaro, G.; Macciantelli, D. *Tetrahedron Lett*. **1977**, *18*, 1079. (e) Forlani, L.; Lunazzi L.; Medici, A. *Tetrahedron Lett*. **1977**, *18*, 4525. (f) Bernardi, F.; Lunazzi, L.; Zanirato, P.; Cerioni, G. *Tetrahedron* **1977**, *33*, 1337. (g) Lunazzi, L.; Magagnoli, C.; Guerra, M.; Macciantelli, D. *Tetrahedron Lett*. **1979**, *20*, 3031. (h) Cremonini, M. A.; Lunazzi, L.; Placucci, G.; Okazaki, R.; Yamamoto, G. *J. Am. Chem. Soc*. **1990**, *112*, 2915. (i) Anderson, J. E.; Tocher, D. A.; Casarini, D.; Lunazzi, L. *J. Org. Chem*. **1991**, *56*, 1731. (j) Gribble, G. W.; Olson, E. R.; Brown, J. H.; Bushweller, C. H. *J. Org. Chem*. **1993**, *58*, 1631. (k) Borghi, R.; Lunazzi, L.; Placucci, G.; Cerioni, G.; Foresti, E.; Plumitallo, A. *J. Org. Chem*. **1997**, *62*, 4924. (l) Garcia, M. B.; Grilli, S.; Lunazzi, L.; Mazzanti, A.; Orelli, L. R. *J. Org. Chem*. **2001**, *66*, 6679. (m) Garcia, M.B.; Grilli, S.; Lunazzi, L.; Mazzanti, A.; Orelli, L. R. *Eur. J. Org. Chem*. **2002**, 4018. (n) Anderson, J. E.; de Meijere, A.; Kozhushkov, S. I.; Lunazzi, L.; Mazzanti, A. *J. Am. Chem. Soc*. **2002**, *124*, 6706. (o) Casarini, D.; Rosini, C.; Grilli, S; Lunazzi, L.; Mazzanti, A. *J. Org. Chem*. **2003**, *68*, 1815. (p) Casarini, D.; Grilli, S.; Lunazzi, L.; Mazzanti, A. *J. Org. Chem*. **2004**, *69*, 345. (q) Bartoli, G.; Lunazzi, L.; Massacesi, M.; Mazzanti, A. *J. Org. Chem*. **2004**, *69*, 821. (r) Casarini, D.; Coluccini, C.; Lunazzi, L.; Mazzanti, A.; Rompietti, R. *J. Org. Chem*. **2004**, *69*, 5746.

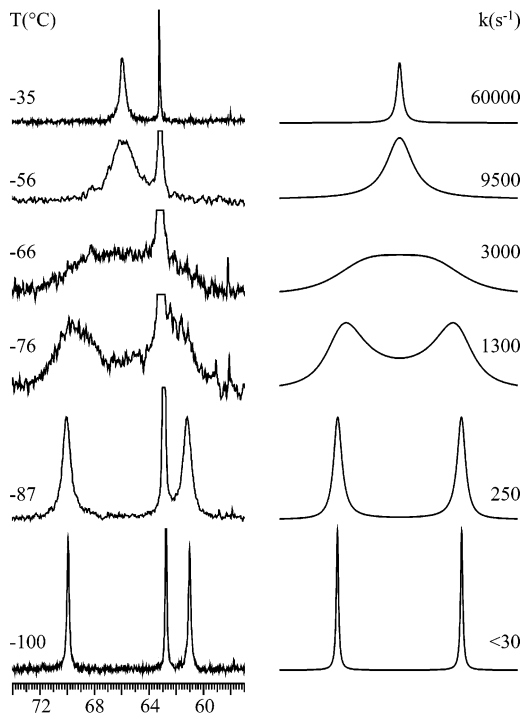

FIGURE 3. Temperature dependence of the ^{13}C signals (150.8 MHz in CD_2Cl_2) of the aliphatic carbons at positions 3,5 and 9b (65.5 and 62.8 ppm at −35 °C, respectively) of compound **1** (left). The line of the single carbon at position 9b is not sensitive to the internal motion and, therefore, was not included in the simulation (right).

TABLE 1. Experimental Values and Computed Ranges for the Vicinal *J* Couplings (Hz) Involving the Hydrogen at Position 9b

	vicinal J_{HCCH}		vicinal J_{HNCH}	
compound	experimental	computed	experimental	computed
1	4.5	4.7 ± 0.5		
2	8.4	8.6 ± 1.5		
1-H^+	4.4	4.4 ± 1.3	8.7	11.5 ± 0.1
2-H^+ (major)	9.2	8.8 ± 1.8	4.9	5.9 ± 1.0
2-H^+ (minor)	5.0	5.2 ± 1.7	11.6	11.8 ± 0.2

The ^{13}C spectrum of **1** (150.8 MHz in CD_2Cl_2) shows a broad signal (ca. 129.5 ppm) for the CH carbons in the *meta* position to OMe (C11); on lowering the temperature (Figure 2), this signal broadens further and eventually splits into a pair of equally intense integrated lines (the same occurs for the C12 line, *ortho* to the OMe group, although with a lower shift separation).

This process is due to the restricted rotation of the aryl rings, and from the rate constants obtained by line shape simulation, a $\Delta G^{\ddagger}$ value of 12.5_5 kcal mol^{-1} was derived[22] (Table 2).

On further lowering the temperature, almost all of the ^{13}C lines broaden, and at −100 °C, they split into pairs; in particular, the aromatic carbons at position 11, which yielded two lines at −36 °C, as shown in Figure 2, exhibit four lines at −100 °C, as do the aromatic carbons at position 12 (Figure S2 of Supporting Information). As an example, the trace of Figure 3 displays the splitting of the line due to the pair of carbons at positions 3,5, whereas the single line of the carbon at position 9b, obviously, does not split. This process is due to the slow inversion of the six-membered rings, which has a free energy of activation of 8.6 kcal mol^{-1} (Table 2), as obtained from the rate constants reported in the simulated spectra

In order to better understand the nature of this inversion process, a search for the corresponding transition state was

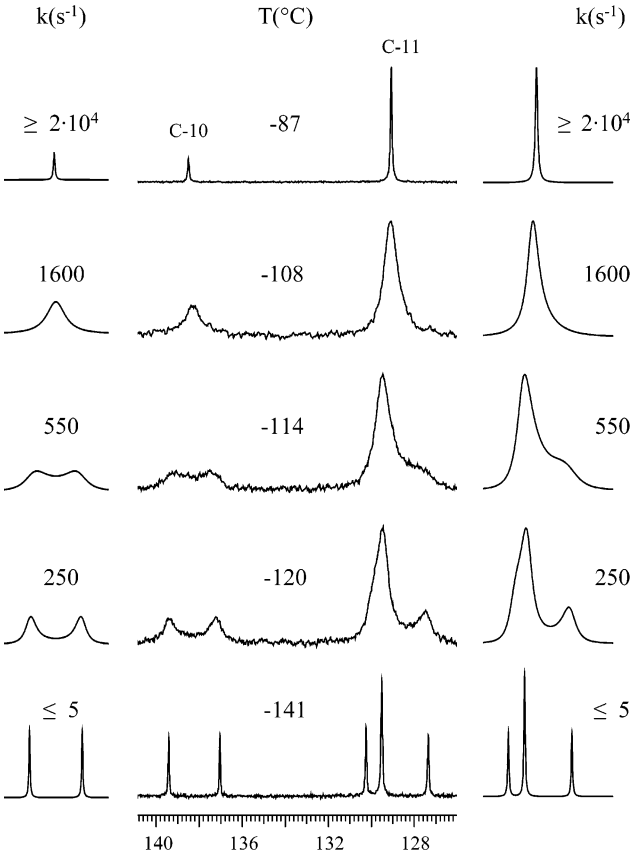

FIGURE 4. Temperature dependence of the ^{13}C signal (150.8 MHz in $CHF_2Cl/CHFCl_2$) of the carbons *para* to the OMe group (C10) of compound **2**, which splits into a 1:1 doublet at −141 °C, whereas that of the carbons *meta* to the OMe group (C11) splits into three lines (1:2:1 ratio) at the same temperature. The simulations were obtained with the rate constants reported.

TABLE 2. Experimental and DFT-Computed Barriers (kcal mol^{-1}) for 1 and 2

	ring inversion		aryl rotation	
compound	experimental	computed	experimental	computed
1	8.6	9.6	12.5_5	14.2
2	7.0	5.6	not measurable[a]	aryl A: 13.3 aryl B: 2.1

[a] See text.

(23) The experimental rate constants are relative to the motion of both the six-membered rings, thus the motion of a single ring corresponds to half the rate constants reported. It is thus the $\Delta G^{\ddagger}$ obtained from 1/2 *k* values that should, in principle, be compared to the theoretical value of 9.6 kcal mol^{-1}. The $\Delta G^{\ddagger}$ obtained in this way (8.9 kcal mol^{-1}) is in even better agreement with the theory. See: Lunazzi, L.; Mazzanti, A.; Minzoni, M. *J. Org. Chem.* **2007**, *72*, 2501.

(24) This process does not correspond to the typical chair to chair inversion (where the axial substituents become equatorial) since here the twist-boat becomes a chair and vice versa (see: Kolossovary, I.; Guisa, W. *J. Am. Chem. Soc.* **1993**, *115*, 2107), keeping the aryl substituents in the pseudoequatorial situation (i.e., *syn* to the five-membered ring).

(25) The degree of pyramidalization is defined as 360°−∑RNR and covers the range of 40 (for a nearly perfect pyramidal nitrogen, as that of NH_3) to 0° (for a perfectly planar nitrogen). In the case of acyclic three-alkyl amines (such as NMe_3), this degree is about 27°, and it is somewhat lower in the case of cyclic three-alkyl amines; see: Ganguly, B.; Freed, D. A.; Kozlowski, M. C. *J. Org. Chem.* **2001**, *66*, 1103.

carried out by means of DFT computations. This structure (reported in Figure S3 of Supporting Information) has a computed energy 9.6 kcal mol^{-1} higher than that of the ground state of Figure 1. Such a value is in fair agreement with the measured barrier[23] and indicates that the transition state corresponds to the transformation of the twist-boat six-membered ring into a chair and vice versa.[24] This process, apparently, does not involve a significant inversion of the nitrogen atom; the latter, in fact, has essentially the same degree of pyramidalization[25] in the ground and in the transition states, with these values being 23.4 and 22.4°, respectively.

Likewise, we used DFT calculations to identify the transition state that accounts for the rotation of the aryl rings. The structure for the corresponding transition state was found to have a computed energy 14.2 kcal mol^{-1} (Table 2) higher than that of the ground state, again in satisfactory agreement with the experimental barrier.[26] These calculations indicate that, in order to make sufficient space to accomplish the rotation of the aromatic rings, a flattening of the nitrogen atom is also required.[27] In this transition state, in fact, the latter is computed to be almost planar, its degree of pyramidalization[25] being 5.2° (see Figure S3 of Supporting Information).

The structure of the isomeric compound **2** was also obtained by means of NOE experiments that indicate the same type of *cis,cis* junction for the perhydrocyclopentaquinolizine moiety since, as in the case of **1**, irradiation of the H9b triplet enhances the signal of the hydrogens at positions 7a,9a (Figure S4 of Supporting Information). Here the two aryl groups are *anti* to the five-membered ring (i.e., in a dynamic pseudoaxial position) since irradiation of the H9b triplet enhances the aromatic hydrogens in a *meta* position to the OMe group (position 11) and yields a very small effect on the signals of H3,H5, contrary to the case of **1** (Figure S4 of Supporting Information).

The two most stable conformers of the above structure[28] were identified by DFT computations,[18] and in Figure 1 (bottom left), the preferred conformation is displayed (its energy being 1.1 kcal mol^{-1} lower than that of the second most stable form, where both of the six-membered rings are chairs). As it appears in Figure 1, the two six-membered rings of the static conformer are different because one is a chair and the other is essentially a boat. Accordingly, the perhydrocyclopentaquinolizine moiety has a different shape than in the case of **1**, and for this reason, the corresponding H−C9b−C9a−H and H−C9b−C7a−H dihedral angles are significantly smaller (i.e., 31 and 3.5°, respectively). From the Karplus equation,[12] the related *J* couplings become 5.9 and 8.2 Hz, respectively, and the average value, resulting from the fast inversion process, is thus 7.0_5 Hz. The direct DFT determination[18] of these couplings yields an average value of 10.1 Hz (resulting from 8.4 and 11.8 Hz). By taking into account these two approaches (that define a range of 7.0_5−10.1 Hz), a vicinal *J* coupling of 8.6 ± 1.5 Hz is predicted (Table 1), in agreement with the experimental value of 8.4 Hz.[29]

Therefore, the structures proposed for **1** and **2** on the basis of the NOE experiments also account for the observation of a vicinal *J* coupling larger in **2** with respect to **1**, although both compounds have the same type of *cis,cis* ring junction.

Like in the case of **1**, the ^{13}C signals of **2** also broaden on cooling and eventually yield a greater number of sharp lines, owing to the restriction of the internal motions. As an example, in Figure 4 is reported the temperature dependence of the signals of the quaternary aromatic carbon in the *para* position to OMe (C10) and of the aromatic CH carbon in the *meta* position to OMe (C11). The carbons at position 10 have the corresponding signal insensitive to the aryl rotation because they lie on the rotation axis of the aryl moiety, thus the observed 1:1 splitting must be attributed solely to the restriction of ring inversion, the corresponding barrier, obtained from the rate constants of Figure 4, being 7.0 kcal mol^{-1}.

The carbons at position 11, on the other hand, have the corresponding signal sensitive to both rotation and inversion processes and should yield, in principle, two doublets (as observed for compound **1**). Contrary to the case of **1**, however, only three lines, with a 1:2:1 intensity ratio, are observed below −140 °C (Figure 4), suggesting that the rotation process of one of the two aryl groups is frozen at this temperature, whereas the other is not. This was confirmed by the observation that the C-12 signal also splits into three lines with the same 1:2:1 intensity pattern. The first and the third lines of C11 in Figure 4 (130.3 and 127.4 ppm, respectively) are those of the two diastereotopic carbons of the aryl group which does not rotate anymore, whereas the two-fold intense central line (129.5 ppm) is that of the two equivalent carbons of the aryl group which is still in the fast rotation mode. The line shape simulation of these three lines was obtained without a direct exchange rate between the first and third line (i.e., the rate corresponding to the aryl rotation); their exchange occurred through the intermediacy of the ring inversion rate, as shown by the fact that the same values of the rate constants used to simulate the exchange of the C10 lines were also employed. This situation, therefore, corresponds to that observed in the cases of exchange processes that, in spite of the presence of a higher barrier, are nevertheless NMR invisible until a second process, with a lower barrier, is also frozen.[30,31] In this case, the rotation of one of the two aryl groups has a barrier higher than ring inversion but can be observed only when the latter process (which is the rate-limiting process) is also frozen; this means that the high rotation barrier cannot be experimentally determined. The lower rotation barrier of the other aryl group, on the other hand, cannot be determined for a different reason, that is, because its value is too low for an NMR measurement. The following computational results help in understanding this type of stereodynamics.

The DFT-computed transition state for the ring inversion process indicates that, in order to transform the chair into a boat

(26) As discussed in ref 15, the barrier for the rotation of a single aryl ring becomes 13.0 kcal mol^{-1}, again in better agreement with the theory (14.2 kcal mol^{-1}).

(27) Such a flattening does not seem to correspond to a nitrogen inversion process, in that the nitrogen atom comes back, apparently, to the same initial pyramidal arrangement.

(28) Actually, there is also a computed minimum with an energy 0.4 kcal mol^{-1} higher than that of the ground state, but this corresponds to a conformer having the same arrangement for the three fused rings shown in Figure 1 and differing solely by the torsion angles of the two aryl groups (62 and 54° rather than 13 and 52°).

(29) Except for the presence of the two OMe groups, compound **2** corresponds to that indicated as **31** (29%) in ref 8a (both have, in fact, very similar NMR parameters for the perhydrocyclopentaquinolizine moiety). On the basis of the present results, the structure of the latter should be therefore corrected and the same structure of compound **2** should be assigned.

(30) Such a situation, for instance, has been encountered in some aliphatic amines where the larger C−N rotation barrier is NMR invisible until the N inversion, which has a lower barrier, is also frozen; see: Jackson, W. R.; Jennings, W. B. *Tetrahedron Lett.* **1974**, *15*, 1837.

(31) (a) Anderson, J. E.; Casarini, D.; Ijeh, A. J.; Lunazzi, L. *J. Am. Chem. Soc*. **1997**, *119*, 8050. (b) Casarini, D.; Lunazzi, L.; Mazzanti, A.; Foresti, E. *J. Org. Chem*. **1998**, *63*, 4746. (c) Lunazzi, L.; Mazzanti, A.; Álvarez Muñoz, A. *J. Org. Chem*. **2000**, *65*, 3200.

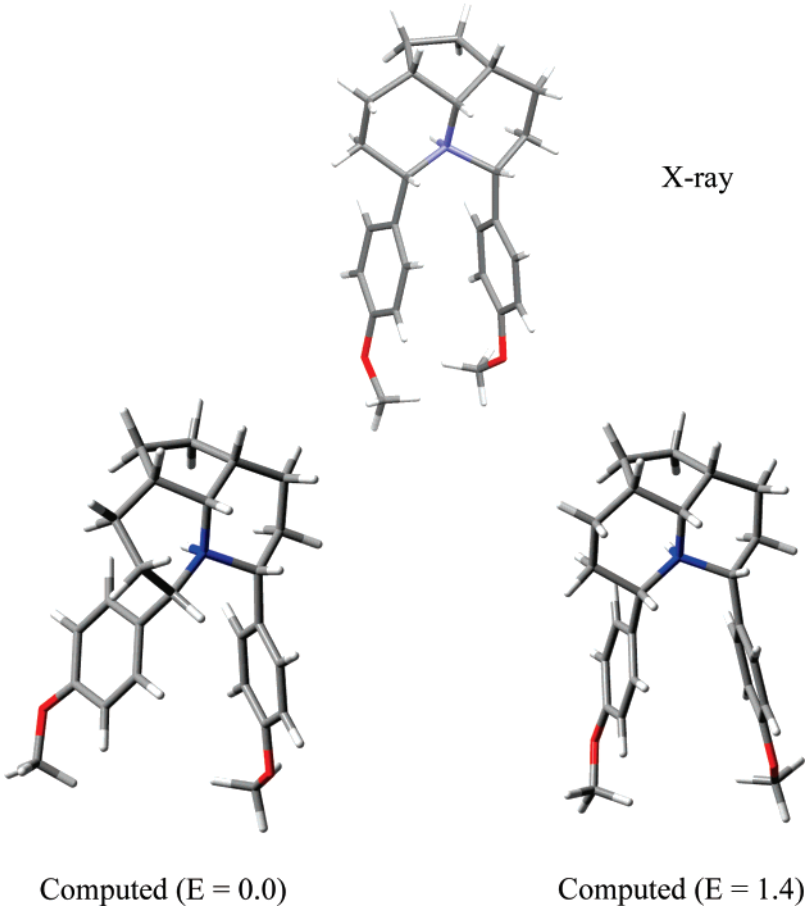

FIGURE 5. Single-crystal X-ray diffraction structure of the ammonium salt **1**-H^+ (top). Underneath are reported the two most stable DFT-computed conformers, with the relative energies (*E*) in kcal mol^{-1}. In the computations, the presence of the CF_3COO^- anion has been neglected for convenience.

(and vice versa), a concomitant nitrogen inversion is also required; in the course of this process, in fact, the nitrogen atom inverts through an essentially planar state having a degree of pyramidalization of 2.2° (see Figure S5 of Supporting Information). The energy for this transition state, computed with respect to the ground state, is 5.6 kcal mol^{-1}, a value lower than that computed (9.6 kcal mol^{-1}) in the case of **1**. This result parallels the experimental determination that yields an inversion barrier for **2** lower than that for **1** (i.e., 7.0 vs 8.6 kcal mol^{-1}, as in Table 2).

In the static conformation of **2** (reported in Figure 1), the two aryl groups (labeled A and B) are in very different positions, contrary to the case of **1**; the rotation transition state of one of them (aryl A in Figure S5 of Supporting Information) is computed to have an energy of about 13.3 kcal mol^{-1} (i.e., similar to that of **1**), while that of the other (aryl B) is only 2.1 kcal mol^{-1}. The latter is too low for an NMR determination, thus one of the two aryl groups will always display, at any attainable temperature, a single line for the corresponding carbons at position 11, as experimentally observed.

Since the inversion barrier of the perhydrocyclopentaquinolizine ring is computed (and measured) to be much lower than 13.3 kcal mol^{-1}, the aryl group A, with the higher rotation barrier, exchanges rapidly its position with the aryl B (which has the 2.1 kcal mol^{-1} rotation barrier). When this rapid A to B exchange has occurred, the rotation of the former aryl A also becomes very fast and, for this reason, cannot display the shift differences for its C11 lines; this will only occur when the ring inversion process, which restores the identity of the aryl A, is also frozen. The kinetic is controlled, in practice, by the process with the lower of the two barriers[30,31] (i.e., ring inversion), so that the higher barrier, for the rotation of aryl A, cannot be determined by NMR (Table 2).

Ammonium Salts 1-H^+ and 2-H^+. When treated with 1 equiv of CF_3COOH, compound **1** yields the corresponding ammonium salt (**1**-H^+). Its NMR spectrum displays essentially the same vicinal coupling (J = 4.4 Hz) as that of **1** for the hydrogen at position 9b, with the latter being, in addition, coupled with the NH^+ hydrogen (J = 8.7 Hz). Also, the patterns of the NOE experiments[32] (Figure S6 of Supporting Infor-

(32) The NOE experiments were carried out at −10°C since the spectrum displays a better resolution than at ambient temperature. This depends on the fact that in a CD_2Cl_2 solution the salt **1**-H^+ appears to experience an exchange process with a form which is present in such a small amount (less than 1%) as to be NMR invisible (possibly the form where the N−H^+ bond is synclinal, rather than antiperiplanar, to the H−C9b bond). At −10 °C, the rate of this process becomes sufficiently slow as to make the lines of the salt sharper than at +25 °C. This is the well-known effect occurring when there is an exchange process between two very biased partners. See: (a) Anet, F. A. L.; Basus, V. J. *J. Magn. Reson.* **1978**, *32*, 339. (b) Okazawa, N.; Sorensen, T. S. *Can J. Chem.* **1978**, *56*, 2737. (c) Lunazzi, L.; Mazzanti, A.; Casarini, D.; De Lucchi, O.; Fabris, F. *J. Org. Chem.* **2000**, *65*, 883. The hypothesis of two forms for such a type of ammonium salt will be better clarified in the case of the ammonium salt **2**-H^+.

mation) parallel those of **1**; the value of the vicinal *J* coupling and the NOE results thus indicate that the salt has the same type of structure as the free amine **1**; that is, the two aryl groups in a pseudoequatorial position are *syn* to the five-membered ring. This structure is confirmed by the single-crystal X-ray diffraction of **1-H**$^+$ (Figure 5, top) that displays a *cis,cis* junction at the perhydrocyclopentaquinolizine moiety, with the NH^+ hydrogen antiperiplanar to the hydrogen at position 9b.

The solid-state conformation of the salt **1-H**$^+$ shows that both of the six-membered rings adopt a chair disposition, whereas the DFT calculations indicate that this corresponds to the second most stable conformer, the preferred one (with a 1.4 kcal mol^{-1} lower energy) being that where one ring is a chair and the other a twisted-boat, like amine **1**. It is not unusual to encounter such differences between the conformations in solids and in solution that depend on the fact that the crystals privilege the conformation which fits better the crystal cell.[33,34]

The conformation adopted in solution, on the other hand, corresponds to that predicted by calculations, as proven by low-temperature NMR spectra. Below +5 °C, the ^{1}H signals of the aromatic hydrogens *meta* to OMe (position 11) decoalesce, in fact, into a pair of signals, as shown in Figure S6 (trace a) of Supporting Information. The aryl rotation barrier responsible for this effect was found to be 12.2_5 kcal mol^{-1} (Table 3), a value essentially equal, within the errors (±0.15 kcal mol^{-1}), to that determined for the amine **1**. On further lowering the temperature, a number of aliphatic ^{1}H and ^{13}C signals broaden and eventually decoalesce at −130 °C, due to the freezing of the ring inversion process; as an example, the splittings of the CH carbons at positions 7a,9a and CH_2 carbons at positions 2,6 are displayed in Figure 6. This feature proves that in **1-H**$^+$ the two six-membered rings are different, as predicted by calculations (i.e., a twisted-boat and a chair), and not equal (two chairs) as in the crystal.

Furthermore, since a N-inversion process cannot occur in the ammonium salt, this finding supports the theoretical prediction that the ring inversion pathway (chair to twisted-boat and vice versa) in amine **1** does not involve appreciable N inversion. The value of the barrier measured for the ring inversion in **1-H**$^+$ (7.7 kcal mol^{-1}, as in Table 3) is quite close to that of the analogous process occurring in **1**, the difference being only 0.9 kcal mol^{-1}.

Also the amine **2** yields the corresponding ammonium salt (**2-H**$^+$) when treated with 1 equiv of CF_3COOH. The corresponding room-temperature spectrum of this salt shows the presence of two forms at the equilibrium; there are, in fact, two spectral traces, with very different intensity, having the line widths broadened by a mutual exchange process. When cooled to −10 °C, in fact, these lines become sharper so that the signal of the minor form could be integrated, indicating that its proportion is 3 ± 0.3% (Figure S7 of Supporting Information).

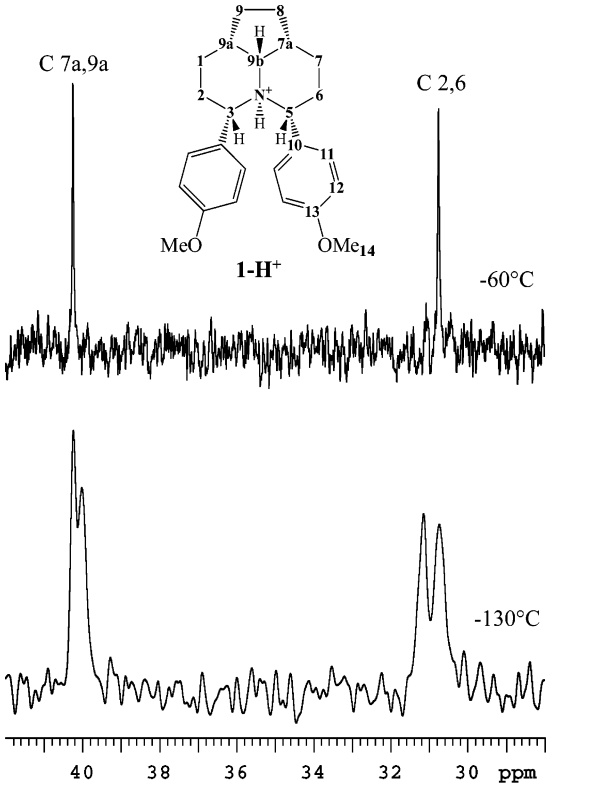

FIGURE 6. Temperature dependence of the ^{13}C signals (150.8 MHz in CD_2Cl_2/CHF_2Cl) of the CH and CH_2 carbons of the ammonium salt **1-H**$^+$ at positions 7a,9a and 2,6.

TABLE 3. Experimental and DFT-Computed Barriers (kcal mol^{-1}) for the Ammonium Salts 1-H$^+$ and 2-H$^+$

	ring inversion		aryl rotation	
compound	experimental	computed[a]	experimental	computed[a]
1-H$^+$	7.7	8.9	12.2_5	19.4
2-H$^+$ (major)	10.1_5	15.0	aryl A: —[b]	aryl A: 16.6
			aryl B: 5.5	aryl B: 7.3

[a] In these computations, the anion CF_3COO^- has not been included. [b] Not measureable, see text.

The sharpening of the lines at lower temperatures is an effect analogous to that observed[32] in **1-H**$^+$; however, the signals of the minor form, although quite small, are clearly visible. The exchange between the two forms of the salt can take place because the H^+ of the N−H^+ bond is quite mobile in solution, so the corresponding bond can be broken at ambient temperature, making it possible for H^+ to be linked to the nitrogen atom in two opposite positions, yielding, as a consequence, a pair of isomeric ammonium salts having the pyramid of nitrogen inverted.

We suggest that the structure of the major form should be that where the N−H^+ bond is in a synclinal relationship with the H−C bond at position 9b, whereas the minor form should correspond to the structure where the N−H^+ bond is antiperiplanar to the H−C9b bond. The DFT-computed structures (Figure S8 of Supporting Information) indicate, in fact, that the former structure (synclinal) is about 6 kcal mol^{-1} more stable[35] than the latter (antiperiplanar).

Experimental support for this assignment was obtained by means of NOE experiments. In particular, irradiation of the H9b signal[36] of the major form yields a very large enhancement of

(33) (a) Johansen, J. T.; Vallee, B. L. *Proc. Natl. Acad. Sci. U.S.A.* **1971**, *68*, 2532. (b) Kessler, H. *Fresenius Z. Anal. Chem.* **1987**, *327*, 66. (c) Burke, L. P.; DeBellis, A. D.; Fuhrer, H.; Meier, H.; Pastor, S. D.; Rihs, G.; Rist, G.; Rodebaugh, R. K.; P. Shum, S. P. *J. Am. Chem. Soc.* **1997**, *119*, 8313. (d) Paulus, E. F.; Kurz, M.; Matter, H.; Vértesy, L. *J. Am. Chem. Soc.* **1998**, *120*, 8209. (e) Coluccini, C.; Grilli, S.; Lunazzi, L.; Mazzanti, A. *J. Org. Chem.* **2003**, *68*, 7266. (f) Perry, N. B.; Blunt, J. W.; Munro, M. H. *Magn. Reson. Chem.* **2005**, *27*, 624.

(34) A situation where it has been unambiguously demonstrated that the X-ray diffraction structure in the solids is that of the minor conformer present in solution has been reported: Lunazzi, L.; Mazzanti, A.; Minzoni, M.; Anderson, J. E. *Org. Lett.* **2005**, *7*, 1291.

the NH^+ signal at 10 ppm (Figure S7 of Supporting Information) since the average interproton distance is computed to be as low as 2.1 Å. On the other hand, irradiation of the signal of the two equivalent H3,H5 hydrogens (Figure S7 of Supporting Information) yields a much lower enhancement of the NH^+ signal; the corresponding average interproton distance is computed to be 2.64 Å, thus entailing an NOE effect smaller by a factor of about 4 with respect to the previous one. Such a result (i.e., the trend of the enhancement of the NH^+ signal) is opposite to that observed for **1**-$\mathbf{H}^+$ (Figure S6, traces b and c), thus reinforcing the conclusion that in the major form of **2**-$\mathbf{H}^+$ the $N-H^+$ and the H−C9b bonds adopt a synclinal, rather than an antiperiplanar, relationship.

Independent support for this assignment is also obtained by the analysis of the vicinal *J* coupling constants (Table 1).[37,38] The major form (97%) of **2**-$\mathbf{H}^+$ displays a $J = 9.2$ Hz for the vicinal coupling[36] between H9b and the H7a, H9a pair (Table 1), that is, a value close to that (8.4 Hz) measured in the corresponding amine **2**. This suggests, therefore, that the salt and the amine have the same type of structure (i.e., a *cis*,*cis* junction) for the perhydrocyclopentaquinolizine moiety, with the two aryl groups *anti* to the five-membered ring in a pseudoaxial position. Indeed, the DFT-computed structure of the lower energy form of **2**-$\mathbf{H}^+$ (Figure S8 of Supporting Information, left) is quite similar to the computed structure of the corresponding amine **2** (Figure 1, bottom).

The solid-state structure of **2**-$\mathbf{H}^+$, obtained by single-crystal X-ray diffraction, is essentially equal to that proposed for the major form in solution (see Figure S8 of Supporting Information), thus confirming that the $N-H^+$ and the H−C9b bonds are in a synclinal relationship and also that one of the two six-membered rings is a chair and the other a boat.

On lowering the temperature, the single ^{1}H signal of the two OMe groups of the major (97%) form broadens and splits into a pair of equally intense lines at −93 °C, as in Figure S9 of Supporting Information (the same occurs for the signal of the hydrogens at positions 3 and 5). Since the signals of these hydrogens are insensitive to the effect of the aryl rotation, the observed dynamic process must be attributed to the restriction of ring inversion. This agrees with the computations that show how the two perhydroquinolizine rings have different shapes in the major form, one being a chair and the other a boat (Figure S8 of Supporting Information). The chair to boat interconversion is fast at ambient temperature (making isochronous the signals of the OMe as well of the H3,H5 hydrogens and carbons) but becomes slow below −90 °C, thus rendering these hydrogens diastereotopic. Line shape simulation yields a barrier of $10.1_5 \pm 0.15$ kcal mol^{-1} (Table 3) for the chair to boat ring inversion.[39]

On the contrary, the OMe signal of the minor (3%) form of **2**-$\mathbf{H}^+$ remains a single line in the same temperature range. This behavior is in keeping with the structure predicted by DFT computations for the minor conformer, where the two perhydroquinolizine rings are equal (both have the shape of a chair as in Figure S8 of Supporting Information), thus in this form, the two aryl rings cannot become diastereotopic.

In the same temperature range, the major form also displays dynamic effects for each of the aromatic doublet signals of the hydrogens in the *ortho* and *meta* positions to the methoxy substituents (H12 and H11, respectively). Both signals eventually split into three doublets with a 1:1:2 intensity ratio (Figure 7), indicating that, in addition to the restricted chair to boat interconversion, the rotation of one of the two aryl groups is also restricted at −93 °C whereas the other is not. This dynamic process is essentially the same as that described above for the corresponding amine **2**.[40] Accordingly, the higher rotation barrier of one aryl group (labeled A in Figure S8 of Supporting Information) is not measurable because the related effects are detectable only when the faster ring inversion is also frozen. On the other hand, the rotation barrier of the second aryl group (labeled B) must be lower than that for the ring inversion.

Proof of the correctness of this interpretation is offered by the ^{13}C spectrum (at 150.8 MHz) in CHF_2Cl. At about −100 °C, in fact, the carbons at position 11 display, as do the corresponding CH hydrogens in Figure 7, three signals (one of which is again twice as intense as the other two), but on further cooling, the two-fold intense signal broadens significantly and eventually splits into two 1:1 lines, separated approximately by 500 Hz at −152 °C. At this temperature, therefore, the rotation of the second aryl group B is also frozen and the corresponding barrier (5.5 ± 0.3 kcal mol^{-1}) is lower, as anticipated, than that measured for the ring inversion. The trend of the computed DFT

(35) The DFT computations were performed, for convenience, on the free cation without including the presence of the anion CF_3COO^-. This might account for the computed energy difference (6 kcal mol^{-1}) being larger than the $\Delta G°$ value (1.9 kcal mol^{-1}), corresponding to the experimental ratio measured at −10 °C.

(36) This signal appears as a multiplet at 3.6 ppm with $J = 9.2$ Hz, due to the coupling with the two equivalent H7a,H9a hydrogens, and $J = 4.9$ Hz, due to the coupling with the NH^+ hydrogen. In the minor form, these *J* values are quite different (5.0 and 11.7 Hz, respectively).

(37) The vicinal *J* coupling between H9b and H7a,H9a, measured in the major form, was found to be larger (9.2 Hz) than that (5.0 Hz) measured in the minor form of **2**-$\mathbf{H}^+$.[36] According to DFT computations, the corresponding dihedral angles of the major asymmetric form of Figure S8 (left) of Supporting Information are 6.6 and 31°, respectively; when inserted in the Karplus equation,[20] they yield a *J* value of 7.0 Hz (resulting from the average of 8.1 and 5.9 Hz, respectively). The angles of the more symmetric minor form, as shown in Figure S8 (right) of Supporting Information, are both equal to 47°, providing a computed *J* value of 3.6 Hz. The direct DFT computation of these vicinal *J* couplings (which include the contribution of the Fermi contact) provides values of 10.6 Hz (average of 13.0 and 8.2 Hz) for the major and 6.9 Hz for the minor form. By combining the two theoretical approaches, the computed coupling of the major form is expected to lie in a 7.0−10.6 Hz range and the minor in a 3.6−6.9 Hz. Thus the major is predicted to have a vicinal *J* coupling (8.8 ± 1.8 Hz) larger than that (5.2 ± 1.7 Hz) of the minor form, in agreement with the trend of the experimental values of 9.2 and 5.0 Hz, respectively (Table 1).

(38) Also, the vicinal $H-N-C-H$ couplings between NH^+ and H9b (4.9 and 11.7 Hz for the major and minor form, respectively[36]) can be rationalized on the basis of the appropriate Karplus-like equation (Fraser, R. R.; Renaud, R. N.; Saunders, J. K.; Wigfield, Y. Y. *Can. J. Chem.* **1973**, *51*, 2433). The corresponding computed dihedral angles for the major (38.5°) and the minor (180°) form yield *J* values of 4.9 and 11.6 Hz, respectively, and the direct DFT computations predict 6.9 and 12.0 Hz, respectively. Thus the $H-N-C-H$ coupling of the major is expected to lie in a 4.9−6.9 Hz range and that of the minor form in a 11.6−12.0 Hz. These values (i.e., 5.9 ± 1 and 11.8 ± 0.2 Hz, as in Table 1) are again in good agreement with the experimental data and further support the proposed assignment.

(39) This value is larger than that measured in the corresponding amine **2**, suggesting that in the ammonium salt the structure is more rigid. This trend is opposite to that observed for the barriers of ring inversion processes in the amine **1** and in its ammonium salt **1**-$\mathbf{H}^+$. The latter, in fact, has a structure quite different from that of **2**-$\mathbf{H}^+$, thus making its shape more flexible than that of the corresponding amine **1**.

(40) The line shape simulation of Figure 7 was obtained using the very same rate constants derived from the simulation of the OMe signal (i.e., the rates corresponding to the chair to boat ring inversion). Furthermore, in order to obtain a good simulation, the rates for the direct exchange between the two downfield signals with a 1:1 intensity could not be included, proving that these signals exchange via the intermediacy of the third signal (that upfield with a double intensity). As discussed in the case of the amine **2**, this proves that the observed motion does not allow the measurement of the rotation barrier but rather the barrier for ring inversion.

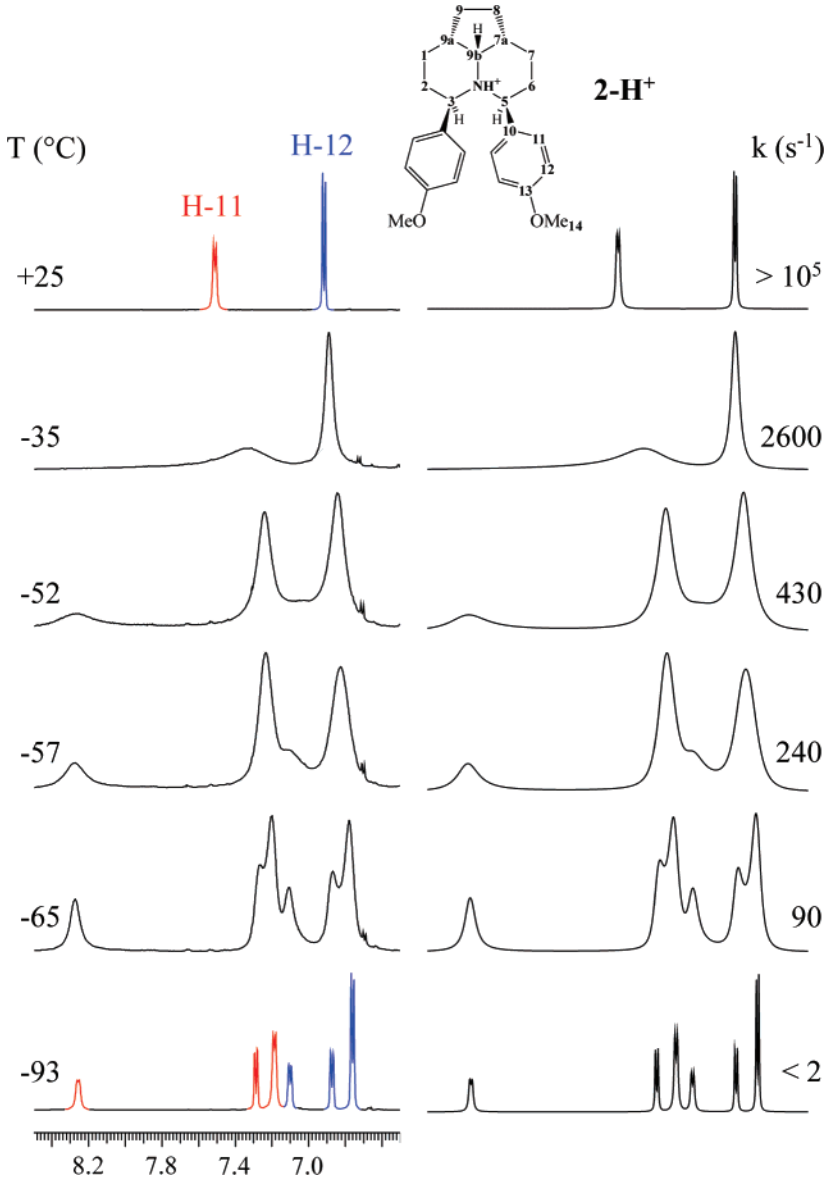

FIGURE 7. Left: Aromatic spectral region (600 MHz in CD_2Cl_2) of the ammonium salt **2**-H^+, where each of the doublet signals of H-11 (red) and H-12 (blue) splits, at −93 °C, into three 1:1:2 doublets. Right: Line shape simulation obtained with the same rate constants derived from those of the OMe line in Figure S9 of Supporting Information (see text). Assignment of the signals was obtained by HSQC acquired at −93 °C (see Figure S10 of Supporting Information).

values for **2**-H^+ (Table 3) agrees with this interpretation since the high and low aryl rotation barriers are 16.6 and 7.3 kcal mol^{-1}, respectively, and the chair to boat ring inversion barrier has an intermediate value (15.0 kcal mol^{-1}).[41]

Concluding Remarks

The structures and conformations of the cyclic amines **1** and **2** were determined by means of NOE experiments, analysis of vicinal *J* coupling constants, and DFT computations. Both display a *cis,cis* junction at the perhydrocyclopentaquinolizine moiety; in the case of **1**, the two six-membered rings adopt the shape of a chair and of a twisted-boat (with the stacked aryl groups displaying a dynamic pseudoequatorial disposition), whereas in the case of **2**, the two six-membered rings adopt the shape of a chair and of a boat (with the stacked aryl groups displaying a dynamic pseudoaxial disposition). The barriers for the ring inversion (8.6 and 7.0 kcal mol^{-1} for **1** and **2**, respectively) and aryl rotation have been determined by dynamic NMR spectroscopy, with values in fair agreement with the theoretical predictions. The corresponding ammonium salts (**1**-H^+ and **2**-H^+) exhibit the same type of structure as well as analogous conformations. The ring inversion barriers were also determined; in the case of **1**-H^+, it was found to be lower (7.7 kcal mol^{-1}) than that of its amine **1**, whereas in the case of **2**-H^+, it was found to be higher (10.1_5 kcal mol^{-1}) than that of its amine **2**. The structures of the two ammonium salts determined in solution (i.e., the *cis,cis* ring junction at the perhydrocyclopentaquinolizine moiety) were also confirmed by single-crystal X-ray diffraction.

(41) The computed barriers of Table 3 are all overestimated, although their sequence does parallel the experimental trend. The main source of approximations in these computations is the consequence of not having considered the presence of the CF_3COO^- anion (in order to reduce the computational time), thus treating **1**-H^+ and **2**-H^+ as "naked" cations.

SCHEME 2

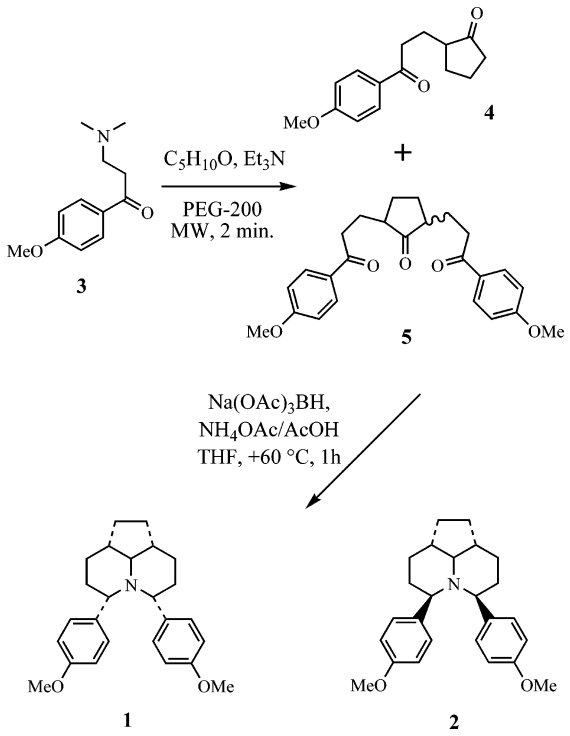

Experimental Section

Material. The isomeric compounds **1** and **2** were prepared following the reaction pathway displayed in Scheme 2.

The Mannich base **3**, prepared from the corresponding Mannich salt,[42] was condensed with cyclopentanone in polyethyleneglycol-200 (PEG-200) under microwave irradiation to provide a mixture of diketone **4** and triketone **5** in a 2.2:1 ratio. The triketone **5**[8a] was obtained as a mixture of *cis*- and *trans*-isomers in an 85:15 ratio. The molecular stitching reductive amination−cyclization of the triketone **5** was next conducted with ammonium acetate and sodium triacetoxyborohydride. This reaction provided (3*S**,5*R**,7a*R**,9a*S**)-3,5-di(4-methoxyphenyl)perhydrocyclopenta[*ij*]quinolizine **1** and (3*R**,5*S**,7a*R**,9a*S**)-3,5-di(4-methoxyphenyl)perhydrocyclopenta-[*ij*]quinolizine **2** in a 7:3 ratio (80% overall yield).

2-[3-(4-Methoxyphenyl)-3-oxopropyl]-5-(3-oxo-3-phenylpropyl)cyclopentan-1-one (5). *β*-Dimethylaminopropiophenone hydrochloride (5 g, 20.5mmol) was taken in a beaker, and the minimum amount of water (10 mL) was added to dissolve the salt. The beaker was kept in an ice bath, and 20% aqueous sodium hydroxide was added dropwise, while periodically checking the pH by means of a pH paper. As neutralization proceeded, the solution became turbid. The addition of sodium hydroxide was continued until the pH reached 10, at which point an oily layer of base was visible. This oily layer was extracted with dichloromethane and concentrated to give *β*-dimethylaminopropiophenone **3** (4.2 g, 20.3 mmol), to which were added cyclopentanone (853 mg, 10 mmol), triethylamine (2.81 mL, 20.28 mmol), and PEG-200 (10 mL) in a 50 mL conical flask. The resulting mixture was irradiated, at atmospheric pressure, in a domestic microwave oven (BPL-Sanyo, India; monomode, multi-power; power source: 230 V, 50 Hz, microwave frequency: 2450 MHz) at 370 W for 2 min. The reaction mixture was cooled to room temperature, diluted with 60 mL of dichloromethane, and poured over ice-cooled water; the organic layer was separated, washed again with water (2 × 50 mL) and saturated aqueous NaCl (50 mL), and dried (Na_2SO_4). The solvent was removed under reduced pressure and the crude mixture separated by column chromatography (silica gel 100−200 mesh, hexane/ethyl acetate 90:10 to 80:20) to give **4** (1.34 g, yield = 26%) and **5**[8a] (4.92 g, yield = 58%).

(3*S,5*R**,7a*R**,9a*S**)-3,5-Di(4-methoxyphenyl)perhydrocyclopenta[*ij*]quinolizine (1) and (3*R**,5*S**,7a*R**,9a*S**)-3,5-Di(4-methoxyphenyl)perhydrocyclopenta[*ij*]quinolizine (2).** To a stirred solution of $NaBH(OAc)_3$ (738 mg, 3.67 mmol) in dry THF (10 mL) were added 2-[3-(4-methoxyphenyl)-3-oxopropyl]-5-(3-oxo-3-phenylpropyl)cyclopentan-1-one **5** (500 mg, 1.22 mmol), ammonium acetate (471 mg, 6.13 mmol), and acetic acid (0.5 mL), in sequence, at room temperature under a blanket of dry nitrogen. The resulting reaction mixture was stirred and placed in a preheated oil bath at 60 °C for 1 h. The mixture was then cooled to ambient temperature, and the pH was adjusted to 7.5 with 20% NaOH (about 8 mL). To the resulting biphasic mixture were added dichloromethane (DCM, 20 mL) and water (5 °C, 25 mL), and the organic layer was separated. The aqueous layer was extracted with dichloromethane (10 mL × 2). The combined organic layer was washed with water (2 × 50 mL) and brine (20 mL) and dried over anhydrous Na_2SO_4. The solvent was removed under reduced pressure and the crude mixture subjected to column chromatography (silica gel 100−200 mesh, hexane/ethyl acetate 97:3 to 90:10) to obtain **1** and **2** in 80% (369 mg) yield and in a 7:3 ratio.

(3*S,5*R**,7a*R**,9a*S**)-3,5-Di(4-methoxyphenyl)perhydrocyclopenta[*ij*]quinolizine (1):** Yield 256 mg (54%); mp (uncorrected) 90−93 °C; R_f (97:3 hexane/ethyl acetate) = 0.52; ^{1}H NMR (600 MHz, CD_2Cl_2, 25 °C, TMS) *δ* 1.51−1.58 (4H, m), 1.65−1.73 (4H, m), 1.79−1.86 (2H, m), 1.98−2.06 (2H, m), 2.14−2.21 (2H, m), 2.86 (1H, t, *J* = 4.5 Hz, H9b), 3.22 (2H, dd, *J* = 6.0, 4.6 Hz, H3,H5), 3.63 (6H, s, OMe), 6.35−6.38 (2H, m), 6.76 (2H, br s); ^{13}C NMR (150.8 MHz, CD_2Cl_2, 25 °C, TMS) *δ* 24.7 (CH_2), 30.7 (CH_2), 31.5 (CH_2), 41.6 (CH, C7a and C9a), 55.9 (CH_3, OMe), 64.7 (CH, C9b), 67.4 (CH, C3, and C5), 112.8 (CH), 130.2 (CH, br), 138.8 (q), 158.3 (q); IR (KBr solution) ν_{max} (neat) 3039, 2911, 2765, 1606, 1479, 965, 845, 785 cm^{-1}; HRMS (EI) *m*/*z* calcd for $C_{25}H_{31}NO_2$ 377.235479, found 377.2354.

(3*R,5*S**,7a*R**,9a*S**)-3,5-Di(4-methoxyphenyl)perhydrocyclopenta[*ij*]quinolizine (2):** Yield 113 mg (26%); mp (uncorrected) 102−105 °C; R_f (97:3 hexane/ethyl acetate) = 0.40; ^{1}H NMR (600 MHz, CD_2Cl_2, 25 °C, TMS) *δ* 1.34−1.42 (2H, m), 1.43−1.50 (2H, m), 1.58−1.68 (4H, m), 1.74−1.80 (2H, m), 1.91−2.10 (4H, m), 3.31 (1H, t, *J* = 8.4 Hz, H9b), 3.73 (6H, s, OMe), 3.87 (2H, t, *J* = 6.8 Hz, H3,H5), 6.76 (2H, m), 7.28 (2H, m); ^{13}C NMR (150.8 MHz, CD_2Cl_2, 25 °C, TMS) *δ* 27.4 (CH_2), 30.0 (CH_2), 31.2 (CH_2), 39.1 (CH, C7a, and C9a), 55.9 (CH_3, OMe), 56.1 (CH, C9b), 60.4 (CH, C3, and C5), 113.8 (CH), 129.3 (CH), 139.0 (q), 158.9 (q); IR (KBr solutions) ν_{max} (neat) 2931, 2816, 1483, 1440, 1129, 761, 707 cm^{-1}; HRMS (EI) *m*/*z* calcd for $C_{25}H_{31}NO_2$ 377.235479, found 377.2355.

(3*S,5*R**,7a*R**,9a*S**)-3,5-Di(4-methoxyphenyl)perhydrocyclopenta[*ij*]quinolizine Trifluoroacetate (1-H$^+$) and (3*R**,5*S**,7a*R**,-9a*S**)-3,5-Di(4-methoxyphenyl)perhydrocyclopenta[*ij*]quinolizine Trifluoroacetate (2-H$^+$).** A CF_3COOH solution (1 M in $CDCl_3$) was added to a $CDCl_3$ solution of **1** (20 mg, 0.053 mmol) directly in the NMR tube. The reaction was followed by acquiring the NMR spectrum after each addition, monitoring the disappearance of the free base signals. When the conversion was complete, the solvent was evaporated and the residue purified by crystallization ($CHCl_3$). The same procedure was applied in the case of **2**. Crystals suitable for X-ray diffraction were obtained by slow evaporation of the solvent ($CHCl_3$ in both cases).

(3*S,5*R**,7a*R**,9a*S**)-3,5-Di(4-methoxyphenyl)perhydrocyclopenta[*ij*]quinolizine Trifluoroacetate (1-H$^+$):** ^{1}H NMR (600 MHz, CD_2Cl_2, −10 °C, TMS) *δ* 1.60−1.67 (2H, m), 1.83−1.98 (6H, m), 2.26−2.36 (2H, m), 2.45−2.53 (2H, m), 2.72−2.81 (2H, m), 3.47 (1H, dt, *J* = 8.7, 4.4 Hz, H9b), 3.61 (6H, s, OMe), 3.79 (2H, ddd, *J* = 10.3, 8.2, 2.9 Hz, H3,H5), 6.34 (4H, br s), 6.54 (2H, br s), 7.57 (2H, br s), 10.04 (1H, br s, NH); ^{13}C NMR (150.8 MHz, CD_2-

(42) *Vogel's Textbook of Practical Organic Chemistry*, 4th ed.; Furnis, B. S., Hannaford, A. J., Rogers, V., Smith, P. W. G., Tatchell, A. R., Eds.; ELBS: London, 1978; p 815.

Cl_2, −10 °C, TMS) δ 24.9 (CH_2), 27.1 (CH_2), 31.6 (CH_2), 41.2 (CH, C7a, and C9a), 55.9 (CH_3, OMe), 73.0 (CH, C3, and C5), 75.9 (CH, C9b), 114.3 (CH), 130.6 (q), 131.4 (CH, br), 159.7 (q), MS (ESI+) *m*/*z* 378[(M − CF_3COO^-)$^+$, 100%]; MS(ESI−) *m*/*z* 113 [CF_3COO^-, 100%].

(3*R,5*S**,7a*R**,9a*S**)-3,5-Di(4-methoxyphenyl)perhydrocyclopenta[*ij*]quinolizine Trifluoroacetate (2-H$^+$):** ^{1}H NMR (600 MHz, CD_2Cl_2, −10 °C, TMS) δ 1.44−1.57 (4H, m), 1.76 (2H, br s), 2.02−2.15 (4H, m), 2.21−2.32 (2H, m), 2.48 (2H, br s), 3.57 (1H, dt, J = 9.2, 4.9 Hz, H9b), 3.63 (minor OMe), 3.77 (6H, s, OMe), 4.17 (2H, br m, H3,H5), 4.43 (minor form, dt, J = 11.6, 5.0 Hz, H9b), 4.80 (minor form, br m, H3,H5), 6.41 (minor form, d, J = 8.9 Hz), 6.90 (4H, d, J = 8.2 Hz), 7.46 (2H, br s), 9.95 (1H, br s, NH); ^{13}C NMR (150.8 MHz, CD_2Cl_2, +25 °C, TMS) δ 25.9 (CH_2, br), 26.5 (CH_2), 31.0 (CH_2), 36.0 (CH, C7a, and C9a), 56.1 (CH_3, OMe), 58.6 (CH, C3, and C5), 63.6 (CH, C9b), 115.1 (CH), 128.4 (q), 130.8 (CH, br), 161.2 (q); MS (ESI+) *m*/*z* 378[(M − CF_3COO^-)$^+$, 100%]; MS(ESI−) *m*/*z* 113 [CF_3COO^-, 100%].

NMR Spectroscopy. The spectra were recorded at 600 MHz for ^{1}H and 150.8 MHz for ^{13}C. Full assignments of the ^{1}H and ^{13}C signals were obtained by bi-dimensional experiments (g-COSY, edited-gHSQC,[43] and gHMBC[44] sequences). The NOE experiments were obtained by means of the DPFGSE-NOE[45] sequence. To selectively irradiate the desired signal, a 50 Hz wide shaped pulse was calculated with a refocusing SNOB shape[46] and a pulse width of 37 ms. Mixing time was set to 0.75 ÷ 1.1 s. The samples for obtaining spectra at temperatures lower than −100 °C were prepared by connecting to a vacuum line the NMR tubes containing the compound and a small amount of C_6D_6 (for locking purpose) and condensing therein the gaseous CHF_2Cl and $CHFCl_2$ (4:1 v/v) under cooling with liquid nitrogen. The tubes were subsequently sealed in vacuo and introduced into the precooled probe of the spectrometer. Low-temperature ^{13}C spectra were acquired with a 5 mm dual probe, without spinning, with a sweep width of 38 000 Hz, a pulse width of 4.9 μs (70° tip angle), and a delay time of 2.0 s. Proton decoupling was achieved with the standard Waltz-16 sequence. A line broadening function of 1−5 Hz was applied to the FIDs before Fourier transformation. Usually 512−1024 scans were acquired. Temperature calibrations were performed immediately before the experiments, using a Cu/Ni thermocouple immersed in a dummy sample tube filled with isopentane, and under conditions as nearly identical as possible. The uncertainty in the temperatures was estimated from the calibration curve to be ±1.0 °C. The line shape simulations were performed by means of a PC version of the QCPE program DNMR 6, no. 633, Indiana University, Bloomington, IN.

Calculations. Computations were carried out at the B3LYP/6-31G(d) level by means of the Gaussian 03 series of programs[18] (see Supporting Information); the standard Berny algorithm in redundant internal coordinates and default criteria of convergence were employed. The reported energy values are not ZPE corrected. Harmonic vibrational frequencies were calculated for all of the stationary points. For each optimized ground state, the frequency analysis showed the absence of imaginary frequencies, whereas each transition state showed a single imaginary frequency. Visual inspection of the corresponding normal mode was used to confirm that the correct transition state had been found. The *J* coupling calculations were obtained at the B3LYP/6-31G(d) level using the program[18] option that includes the Fermi contact contribution.

Acknowledgment. L.L. and A.M. received financial support from the University of Bologna (RFO) and from MUR-COFIN 2005, Rome (national project "Stereoselection in Organic Synthesis"). H.S.P.R. thanks University Grants Commission (UGC), India, for Special Assistance Program (SAP-DRS), and Council of Scientific Industrial Research (CSIR), India, and the Department of Science and Technology, India (DST-FIST), for financial assistance. S.R. thanks CSIR for the Junior Research Fellowship in the major research project awarded to H.S.P.R. We thank Sophisticated Instrumentation Facility (SIF) and Sophisticated Analytical Instrumentation Center (SAIC) for generously recording preliminary 400 MHz NMR spectra.

Supporting Information Available: Additional variable-temperature spectra, DFT-computed structures, NOE spectra for **1**, **2**, **1-H**$^+$, and **2-H**$^+$, X-ray diffraction data for **1-H**$^+$ and **2-H**$^+$, ambient temperature ^{1}H, ^{13}C NMR, and selected 2D spectra, computational data, and *J* coupling matrix for **1**, **2**, **1-H**$^+$, and **2-H**$^+$. This material is available free of charge via the Internet at http://pubs.acs.org.

JO702172U

(43) (a) Bradley, S. A.; Krishnamurthy, K. *Magn. Reson. Chem.* **2005**, *43*, 117. (b) Willker, W.; Leibfritz, D.; Kerssebaum, R.; Bermel, W. *Magn. Reson. Chem.* **1993**, *31*, 287.

(44) Hurd, R. E.; John, B. K. *J. Magn. Reson.* **1991**, *91*, 648.

(45) (a) Stott, K.; Stonehouse, J.; Keeler, J.; Hwand, T.-L.; Shaka, A. J. *J. Am. Chem. Soc.* **1995**, *117*, 4199. (b) Stott, K.; Keeler, J.; Van, Q. N.; Shaka, A. J. *J. Magn. Reson.* **1997**, *125*, 302. (c) Van, Q. N.; Smith, E. M.; Shaka, A. J. *J. Magn. Reson.* **1999**, *141*, 191. (d) See also: Claridge, T. D. W. *High Resolution NMR Techniques in Organic Chemistry*; Pergamon: Amsterdam, 1999.

(46) Kupče, E.; Boyd, J.; Campbell, I. D. *J. Magn. Reson., Ser. B* **1995**, *106*, 300.